Sequence, Structure, and Function of DNA-Binding Protein in *Deinococcus Wulumuqiensis* R12

Yao Chen
Nanjing Tech University
Zhihan Yang
Nanjing Tech University
Xue Zhou
Nanjing Tech University
Mengmeng Jin
Nanjing Tech University
Zijie Dai
Nanjing Tech University
Dengming Ming
Nanjing Tech University
Zhidong Zhang
Nanjing Tech University
Liying Zhu
Nanjing Tech University
Ling Jiang (jiangling@njtech.edu.cn)
Nanjing University of Technology https://orcid.org/0000-0001-6625-5557

Research Article

Keywords: Deinococcus wulumuqiensis R12, DNA-binding protein, oxidative stress, proteomics, Escherichia coli, E. coli

Posted Date: December 28th, 2021

DOI: https://doi.org/10.21203/rs.3.rs-1142206/v1

Abstract

Deinococcus wulumuqiensis R12, which was isolated from arid irradiated soil in Xinjiang province of China, belongs to a genus *Deinococcus* that is well-known for its extreme resistance to ionizing radiation and oxidative stress. The DNA-binding protein Dps has been studied for its great contribution to oxidative resistance. To explore the role of Dps in *D. wulumuqiensis* R12, the Dps sequence and homologous structure were analyzed. In addition, the *dps* gene was knocked out and proteomics was used to verify the functions of Dps in *D. wulumuqiensis* R12. Docking data and DNA binding experiments *in vitro* showed that the R12 Dps has a better DNA binding ability with the N-terminal than the R1 Dps1. When the *dps* gene was deleted in *D. wulumuqiensis* R12, its resistance to H_2O_2 and UV rays was greatly reduced, and the cell envelope was destroyed by H_2O_2 treatment. Additionally, the qRT-PCR and proteomics data suggested that when the *dps* gene was deleted, the *catalase* gene was significantly down-regulated in cells. And the proteomics data indicated the metabolism, transport and oxidation-reduction processes in *D. wulumuqiensis* R12 were down-regulated after the deletion of *dps* gene. Dps protein might play an important role in *Deinococcus wulumuqiensis* R12.

Introduction

In 1956, a bacterium that had survived exposure to an extremely high dose of ionizing radiation (IR) was accidentally discovered as a contaminant in a can of supposedly to sterilized meat [1]. Now well-known as *Deinococcus radiodurans*, it is one of the most radiation-resistant organisms known to science [2–3]. It is not only tolerant to gamma radiation, but also to other DNA damage and oxidative stress-generating conditions such as UV, desiccation, or high temperature [4–6]. The radiation tolerance of *D. radiodurans* can reach to 15,000 Gy [7], which is 100-fold that of typical microorganisms, 250-fold that of *Escherichia coli*, and 3000-fold that of humans [8–9]. Therefore, *D. radiodurans* is an ideal model strain for studying the oxidative stress response and radiation resistance [10–11].

Several studies have investigated the remarkable oxidative resistance mechanisms of this bacterium, which can be divided into three categories: DNA self-repair [4]; efficient cell evolution mechanism [10]; and effective scavenging of reactive oxygen species (ROS) [11–13]. The DNA repair system of *D. radiodurans* has been identified as a major determinant of its IR resistance. Intermediate dose of IR can cause death to most cells due to numerous double strands broken [4]. However, studies have shown that the protein damage is just as important as the DNA damage following exposure to IR. Daly et al. also put forward the viewpoint of proteomes are important macromolecule that can be affected by IR [14]. The powerful antioxidative system is another determinant of stress resistance in *D. radiodurans* [4]. To adapt to the oxygen-enriched environment of irradiated soil and remove the resulting ROS, microorganisms have evolved various ROS scavenging systems [4, 10]. Notably, *D. radiodurans* has several unprecedented antioxidative systems to protect itself from oxidative stress that are not found in other microorganisms [4]. Among them, DNA-binding protein (Dps), a conserved protein found in most bacterial species, has been devoted a great deal of attention, since it is a vital factor that protects DNA from various oxidative damage in stressed or starved cells [3, 15–16].

Recent studies have painted a clearer picture of the two mechanisms through which Dps exerts its protective in cells: (1) Dps can effectively bind DNA, thereby protecting DNA from the attack of oxygen free radicals [17]; (2) The ferroxidase activity is the key feature of Dps that prevents the formation of highly toxic ROS from the reaction of iron (II) with hydrogen peroxide or dioxygen [18]. Dps can also be oxidized to protect DNA from a distance by DNA charge transfer (CT), which may be another effective DNA protection mechanism [19]. The *dps* gene is also critical for cell survival under stress conditions [20]. When the *dps* gene was knocked out in *Salmonella enterica*, the mutant was more sensitive to antibiotics than the parental strain [21]. Similarly, the *Δdps* mutant of *Riemerella anatipestifer*, was more sensitive to H_2O_2 under iron-rich conditions [22]. However, there are no studies have shown changes in the antioxidant capacity of *Δdps* mutant in genus *Deinococcus*.

The genus *Deinococcus* is interesting because many of its members exhibits extreme radioresistance [23]. *D. radiodurans* R1 was the first strain in this family isolated from canned meat which shows extraordinary resistance to IR [24–25]. *D. Wulumuqiensis* R12 is a member of *Deinococcus* family which was previously isolated by our team from a radiation-contaminated area of Xinjiang Uigur Autonomous Region of northwest China. Strain *D. Wulumuqiensis* R12 is a Gram-positive, reddish orange, non-spore-forming coccus, and its gamma radiation resistance was more than 10 kGy and UV resistance was over 700 J m^{-2} [26]. The *D. Wulumuqiensis* R12 shows higher tolerance for gamma radiation and UV light than that of in *D. radiodurans* R1, and the genome of R12 was also sequenced in our previous work [26]. The R12 genome revealed a single *dps* gene of 645 bp size. Dps is a classic antioxidant protein in organisms. With the aim of shedding some light on the role of Dps in extremophilic genus *Deinococcus* (strain R12), in this study, we constructed a *Δdps* R12 mutant of strain R12 through homologous recombination and subjected it to UV and H_2O_2-induced oxidative stress to investigate the properties and protective function of Dps in *D. Wulumuqiensis* R12. Finally, proteomics analysis was utilized to examine the role of Dps on a wider, systemic level. The results showed that after the deletion of *dps* gene, the antioxidative capacity was reduced, and the envelope was more easily destroyed after H_2O_2 treatment. Finally, the proteomic data revealed that the *dps* gene and Dps protein might affect metabolism, transport, and cell wall etc..

Materials

The *dps* gene was knocked out in *D. wulumuqiensis* R12 which was preserved in our laboratory, using the pK18mobSacB shuttle plasmid from Miaoling Biotechnology Co., Ltd (Wuhan, China). *E. coli* DH5α (Vazyme, Nanjing, China) was utilized for gene cloning. T4 DNA ligase, Phanta DNA polymerase, *Eco*R, *Bam*H were purchased from Vazyme (Nanjing, China). Triton X-100, protease inhibitor, TEAB (tetraethylammonium bromide), trypsin, DTT (dithiothreitol), and IAA (iodoacetamide) were from Sangon (Shanghai, China). Yeast extract and tryptone were purchased from Oxoid (UK). Formic acid, acetonitrile, actone, and other chemicals were from Sigma-Aldrich (Shanghai, China). Tryptone glucose yeast (TGY) medium (5 g/L tryptone, 3 g/L yeast extract, and 1 g/L glucose, pH 7.0) was used for *D. wulumuqiensis* R12 culture. Nutrient agar (NA) medium (10 g/L tryptone, 3 g/L beef extract, 5 g/L NaCl, and 15 g/L agar) was utilized for preparation and transformation of competent cells. Luria-Bertani (LB)

medium (5 g/L yeast extract, 10 g/L tryptone, and 10 g/L NaCl, pH 7.0) was used for *E. coli* DH5α culture. When needed, 1.5% agar was added to obtain a solid medium.

Model building of R1 / R12 Dps and protein/DNA docking

The R12 Dps structure was modeled using RoseTTAFold, and the N- terminal of R1 Dps structure (PDB code: 2C2F) was repaired using the same method. The structures were presented and analyzed using PyMol.

The DNA model was downloaded from PDB. The protein/DNA docking was carried out using Autodock 4.2.6, and the complex with lowest energy was obtained.

Plasmid construction

The primers used in this study are listed in Table S1 and the *D. wulumuqiensis* R12 genome was used as the template. The PCR temperature program was as follows: 1 cycle of 300 s at 98 °C, 35 cycles of 60 s at 98 °C, 60 s at 62.5 °C, 60 s at 72 °C, 1 cycle of 600 s at 72 °C. The temperature program of gene splicing by overlap extension PCR (SOE PCR) as follows: 1 cycle of 300 s at 94 °C, 35 cycles of 20 s at 94 °C, 60 s at 61 °C, 30 s at 72 °C, 1 cycle of 600 s at 72 °C. The amplified fragments and pK18mobSacB plasmid were digested with *Eco*RⅠ, *Bam*HⅠ for 4 h at 37 °C, purified and ligated with T4 ligase at 4 °C for 12 h.

The R12 *dps* gene was amplified from the R12 genome, and the primers were listed in Table S1. The PCR temperature program was as follows: 1 cycle of 300 s at 95 °C, 35 cycles of 15 s at 95 °C, 15 s at 65 °C, 60 s at 72 °C, 1 cycle of 600 s at 72 °C. The R12 *dps* fragments were extracted using “FastPure Gel DNA Extraction Mini Kit (Vazyme)”. The purified fragments were digested by *Nde*Ⅰ, *Xho*Ⅰ, and using T4 ligase to obtain the recombinant plasmid. The R1 Dps1 gene was using the same method to construct the recombinant plasmid.

Expression and purification of the R12 Dps and R1 Dps1 protein

The R12 Dps and R1 Dps1 were expressed in *E. coli* BL21 (DE3) for protein expression. The recombinant strains were cultured in 50 mL LB medium at 37 °C and 200 rpm till the OD_{600} reached to 0.6-0.8. Then, the final IPTG concentration was 0.5 mM was added to the cultures to induce the protein expression in the 200 rpm for overnight at 20 °C.

The cells from 50 mL culture were harvested by 8,000 ×*g* centrifugation for 5 min, and the discarded the supernatants. Then, the cells were resuspended with 3 mL PBS buffer. The cells were disrupted by 300 W sonication for 15 min, and centrifuged at 10,000 ×*g* for 20 min at 4 °C. The supernatants were obtained and loaded onto 1 mL Ni-NTA resin to purify proteins that was pre-equilibrated with 5 mL buffer A (pH 8.0) that contains 20 mM imidazole and 300 mM NaCl. Then 5 mL buffer A was used to remove miscellaneous proteins. Finally, 3 mL buffer B (pH 8.0) contains 300 mM imidazole and 300 mM NaCl was used to elute the target proteins. The supernants and purified proteins were analyzed by SDS

polyacrylamide gel electrophoresis (SDS-PAGE), and the protein concentration was measured ultramicro spectrophotometer (Colibri, Germany).

Construction and screening of the *Δdps* knockout strain

The positive recombinant colonies grown on NA plates containing kanamycin were transferred into TGY liquid medium without antibiotics, and cultured for 2-3 days at 31 °C. Then, 500 μL of the resulting culture were plated onto TGY solid medium containing 10% sucrose and cultured at 31 °C for 3-5 days. Single colonies without bacteriolysis on sucrose TGY solid medium were streaked onto TGY solid medium with and without kanamycin, respectively. Then, clones that grew on TGY solid medium without kanamycin and did not grow on TGY solid medium with kanamycin were transferred into TGY liquid medium without antibiotics and cultured for 2-3 days at 31 °C. Finally, the genomic DNA was extracted using a commercial kit (Takara, china), and the *Δdps* R12 mutant was verified by PCR amplification and sequencing.

The DNA protection of R12 Dps and R1 Dps1 protein

The pET-22b-R12-Dps and pET-22b-R1-Dps1 recombinant plamids were constructed, the used primers were listed in Tablse S1. The 40 μM purified R12 Dps and R1 Dps1 protein in double distilled water and crosslinker fluid (pH 8.0 20 mM phosphate buffer with 80 mM NaCl and 0.1% glutaraldehyde) incubated in room temperature for 30 min, respectively. Then, mix 10 μL pET-22b plasmids (60 ng/μL) and 10 μL 40 μM R12 Dps or R1 Dps1 protein were incubated in room temperature for 30-60 min. The 30 ng/μL plamisds were using as control. Finally, agarose gel electrophoresis was utilized to verify the protection of Dps proteins.

Validation of calatase expression by qRT-PCR

The WT R12 strain and *Δdps* R12mutant was grown in TGY medium at 31 °C for three days. The 4 mL cells were harvested by centrifugation at 12000 ×*g* for 3 min. The total RNA was used bacteria total RNA isolation kit (Sangon, Shanghai). The cDNA was obtained using one-strp gDNA removal and cDNA synthesis supermix (TransGen Biotech, Beijing). The real-time PCR was carried out in Roche LightCycler96 real-time fluorescence quantitative PCR instrument. 16S rRNA was used as internal reference gene. The primers using in this test listed in Table S1. Excel was used to calculate student's *t*-test.

Growth curve analysis of WT R12 strain and *Δdps* R12 mutant

The WT R12 strain and *Δdps* R12mutantatthe logarithmic growth stage were transferred into 50 mL of TGY liquid medium, an inoculation amount of 2%, after which the OD_{600} value was measured every 2 h. Each sample was measured in triplicate and the mean value was recorded.

Survival rate of WT R12 strain and *Δdps* R12 mutant under oxidative stress

The *Δdps* R12mutant was cultured for 48 h in TGY liquid medium at 31 °C. The resulting seed culture was used to inoculate, fresh TGY medium to an initial OD_{600} of 0.6-0.8. Next, the cells were treated with 80 mM H_2O_2 for 0, 10, 20, 30, and 50 min at 31 °C and 800 rpm inheating block. After the stress treatment, 100 μL (10^9 CFU) aliquots of serial 10-fold dilutions (10^{-1}-10^{-5}) of cells were plated onto TGY agar and grown at 31 °C for 3 days. The survival rate was calculated based on the number of colonies in the treated samples compared with the untreated sample (control group). The 10^{-5} dilution was plated onto TGY agar to calculate the number of colony-forming units (CFU) in triplicate.

Survival rate of WT R12 strain and Δdps R12 mutant after exposed to UV irradiation

The *Δdps*R12mutant was cultured to the stationary stage and diluted in a 10^6-fold gradient. Then, 200 μL (10^6 CFU) of the diluted cell suspension were plated onto TGY agar, exposed to 0, 3, 6, 9 and 12 min 700 J m^{-2} UV irradiation, and cultured for 2-3 days at 31 °C. The survival rate was calculated after counting the the colonies. Each group included three independent repeats. The WT R12 strain was included under the same conditions as the control group.

Transmission electron microscopy (TEM)

The WT R12 strain and *Δdps* R12 mutant were grown in TGY liquid medium at 31 °C from starting OD_{600} value reached to 0.6-0.8, at which point they were treated with 80 mM H_2O_2 for 30 min 31 °C. Then, the cells were washed twice with PBS and collected by centrifugation at 12,000 ×*g* for 2 min. The cells were fixed overnight at 4 °C with 2.5% glutaraldehyde, harvested by centrifugation at 4000 ×*g* for 5 min, and embedded in 2% agarose. The slices were stained with uranyl acetate for 15 min and observed under a Hitachi H-7650 transmission electron microscope.

Protein extraction and digestion

The 200 μg samples (which the strains grown to OD_{600} 0.8 were used as samples) were shock frozen -80 °C. A proper of cells was weighed into a pre-cooled mortar, and liquid nitrogen was added. Then, 4 times the volume of lysis buffer (1% Triton X-100 and 1% protease inhibitor) was added to each sample. The cells were disrupted by sonication (240 W) for 15 min. After centrifugation at 12000 ×*g* for 10 min, the supernatant was transferred to a fresh centrifuge tube and the protein concentration was determined using a BCA assay kit (Sangon, Shanghai, China). An equal amount of each sample was subjected to enzymatic hydrolysis, and the volume was adjusted with lysis buffer. Then, 1 volume of pre-cooled acetone was added and vortexed, after which 4 times of pre-cooled acetone was added. The precipitation took place at -20 °C for 2 h. After centrifugation at 4,500 ×*g* for 5 min, the supernatant was discarded and the precipitate was washed twice with pre-cooled acetone. After drying and precipitation, TEAB with a final concentration of 200 mM was added, followed by ultrasonic dispersion of the precipitate. Trypsin was added at a ratio of 1:50 (protease: protein, m/m) and enzymatic hydrolysis was conducted overnight. DTT was added to a final concentration of 5 mM and incubated at 56 °C for 30 min. Then, IAA was added to a final concentration of 11 mM and incubated at room temperature in the dark for 15 min. Finally, the

peptides were desalted by C18 SPE column. Each strain was acquired for triplicate, and each sample was treated as described above.

Liquid Chromatography-Mass Spectrometry/Mass Spectrometry (LC-MS/MS) analysis

The peptide segments were separated on NanoElute in UPLC (Bruker Daltonics) mobile phase A and then separated using a NanoElute ultra-high performance liquid phase system. Mobile phase A was water with 0.1% formic acid and 2% acetonitrile. Mobile phase B was acetonitrile with 0.1% formic acid and 100%. The mobile phase gradient settings were as follows: 0-70 min, 4-22% B; 70-84 min, 22-30% B; 84-87 min, 30-80% B; 87-90 min, 80% B. The flow rate maintained at 450 nL/min. The peptide segments were separated by UPLC and then ionized by injecting into the capillary ion source. The peptide segments were analyzed using a timsTOF Pro (Bruker Daltonics) mass spectrometry instrument. Mass spectrometry data was acquired by Bruker Compass HyStar (Version 5.1.8.1), and analyzed by MaxQuant 1.6.6.0. The voltage of the ion source was set at 1.75 kV, and the parent ion of the peptide segments and its secondary fragments were detected and analyzed using high-resolution TOF scanning. The scanning range of secondary mass spectrometry was set to 400-1500 m/z. The data acquisition was conducted in parallel cumulative serial fragmentation (PASEF) mode. After one set of first-order mass spectrometry data was collected, secondary spectrographs with the charge of the parent ion in the range of 0-5 were collected in PASEF mode 10 times. The dynamic elimination time of tandem mass spectrometry scanning was set to 30 s to avoid repeated scanning of the parent ion.

In our results, at least one razor or unique peptide of a protein was to be considered as identified, the minimum score of peptides was set as 40, and false discovery rate (FDR) was set as 1% to ensure the identities are authentic. FDR is a measure of the incorrect peptide spectral matches (PSMs) among all accepted PSMs [27-29]. Proposed by Benjamini and Hochberg [30] as an alternate to the Bonferroni correction, it is defined as the rate of false positives in accepted hits. FDR is a less stringent metric for global confidence assessment. In the context of proteomics, it is a global estimate of the false positives present in the results obtained by a database search algorithm [31].

Differential protein screening

Protein difference analysis first picks out the samples to be compared, calculates the quantitative mean protein of the repeated samples, and finally the difference multiple of the comparison group was calculated. The calculation formula is showed in . In order to judge the significance of the difference, T-test was carried out for the relative quantitative value of each protein in the two comparison samples, and the corresponding *P* value was calculated, which was taken as the significance index. The default *P* value was ≤ 0.05. To make the test data conform to the normal distribution of the T-test requirements. Before testing, the relative quantitative values of proteins need to undergo Log2 logarithmic conversion. The calculation formula is showed in β. Through the above difference analysis, when *P* value ≤ 0.05, the change of differential expression level over 1.5 was regarded as the change threshold of significantly up-regulated, and less than 1/1.5 was regarded as the change threshold of significantly down-regulated. The

summary data of all differentially expressed proteins in this project are shown in “MS_identified_information” (Supporting information).

:

$$FCA/B, k = Mean(Rik, i \in A) / Mean(Rik, i \in B)$$

β: [P {ik}=T.test(Log2(P {ik},i\in A),Log2(P {ik}, i\in B))\]

A and B were the sample, R represents the relative quantity of protein, i represents the sample, and k represents the protein.

GO and KEGG enrichment analyses

The GO and KEGG enrichment analyses were performed using Blast2go (version 5.2, Biobam, Valencia, https://www.blast2go.com/) and DAVID (version 6.8, https://david.ncifcrf.gov), respectively. GO terms and KEGG pathways with corrected *P*-values of less than 0.05 were considered to be significantly enriched for differentially expression proteins.

Protein-protein interaction prediction

The number of sequences of the differentially expressed-proteins screened according to the fold change over 1.5 in different comparison groups was compared with the protein network of the STRING database (v.11.0), and the interaction of the differentially expressed proteins were extracted according to the confidence score > 0.7 (high confidence). The “Cytoscape” software was used to visualize the interaction network of differentially expressed proteins.

Results And Discussion

Sequence and structure analyses of *D. wulumuqiensis* R12 Dps

To explore the function of *D. wulumuqiensis* R12 Dps, the sequence and structure were analyzed. Through sequence alignment, Dps1 from *Deinococcus radiodurans* R1 (PDB code: 2C2F and the N-terminal was missing) with the highest identity (81.31%), and the alignment between R12 Dps and R1 Dps1 sequences was carried out. The alignment result showed that the N-terminal sequences of R1 Dps1 nad R12 Dps were unconservative, that might play an important role in function differences. The recent research articles have reported that Dps proteins from *E. coli* have identified the N-terminal lysine residues are involved in DNA binding [32].

In order to verify the function of R12 Dps protein N-terminal. The R12 Dps model was built through RoseTTAFold. The N-terminal of R1 Dps1 crystal structure was too flexible that can not be analyzed, therefore, RoseTTAFold was used to repair the structure. Furthermore, the protein/DNA docking was

carried out through AutoDock 4.2.6. The docking result showed that the DNA binding ability of R12 Dps was better than that of R1 Dps1. The Lys3, Ser8, Ser20, Lys20, Asp22, Ser129 and Ala132 residues bond to DNA by hydrogen bonds in R12 Dps/DNA docking result. And in R1 Dps1/DNA docking result, only Thr22 bonds to DNA.

Purification of Dps proteins, DNA binding and protection tests

The docking results showed that R12 Dps DNA binding ability was better than that of R1 Dps1. The DNA binding tests need to verify this computational result. The *dps* gene was amplified from *D. wulumuqiensis* R12 genome, and the recombinant plasmid pET-22b(+)-R12Dps was constructed and expressed in *E.coli* BL21 (DE3). The same method was utilized to obtain the pET-22b(+)-R1Dps1 plasmid which the template was *D. radiodurans* R1 genome. The SDS-PAGE result (Fig. 2C) showed that R1 Dps1 and R12 Dps proteins can be successfully expressed and purified *in vitro*. The molecule weight of R1 Dps1 was ~24 kDa, and the R12 Dps was ~25 kDa, which were consistent with the theoretical molecular weights.

As shown in Fig. 2A, the plasmids (pET-22b) appeared superhelical *in vitro*. The superhelical level of plasmids was reduced with the addition of R1 Dps1 protein or R12 Dps proteins. Compare with the superhelical level between R1 Dps1 and R12 Dps proteins, the lower superhelical level the R12 Dps reflected, indicating the DNA binding ability of the R12 Dps was truly better than R1 Dps1 that confirmed to the docking data.

The Dps protein can combine Fe^{2+} ions to prevent fenton reaction [4]. Therefore, 80 mM and 200 μM $FeSO_4$ were added to plasmids. As shown in Fig. 2B, the plasmids have been destroyed without the addition of Dps proteins, while the plasmids combined with the R1 Dps1 or R12 Dps proteins were remained few plasmids, indicating that the Dps protein can combine Fe^{2+} that the fenton reaction can be prevented. Also, the bromophenol blue was oxidized to yellow under fenton reactions, and the solution which was added Dps proteins that was remain the blue color, demonstrating that the Dps protein can combine Fe^{2+}.

Knockout of the *dps* gene in *D. wulumuqiensis* R12

In order to explore the specific functions of Dps in *D. wulumuqiensis* R12, the *dps* gene was knocked out through homologous recombination. In this study, the suicide plasmid pK18mobSacB was utilized as the bifunctional screening vector with kanamycin resistance gene as a positive selection marker, and the *sac*B gene which encodes a secretory levansucrase as a negative selection marker. The recombinant plasmid was used to knock out the *dps* gene through homologous recombination in *D. wulumuqiensis* R12 as shown in Fig. 3A.

The initial screening was conducted on kanamycin plates to obtain the strains containing the recombinant plasmids (Fig. 3B). Then, the secondary screening was carried out, and the single colonies were selected from the sucrose NA plate and streaked onto TGY plates with or without kanamycin respectively to obtain the strains which has been cured of the recombinant plasmid without marker

genes. Clones that grew on the NA plate without kanamycin but not on kanamycin were selected. The genomic DNA of the rescreened knockout and WT R12 strains as isolated, and homologous primers were used for PCR amplification. The genomes of wild-type R12 and *Δdps* R12 mutant were extracted and sequenced, the sequencing primers were homologous arm F1 and R2, the sequencing result showed that 784 bp which contain *dps* gene was knocked out in the *Δdps* R12 mutant genome (Fig. S1). Here, the target we designed to replace contains extra 139 bp on the both sides of the *dps* gene (645 bp) to ensure the target gene was successful knockout. Therefore, the final fragments deleted in the genome contains totally 784 bp. Finally, the PCR products which used primers F1, and R2 (Table S1) to amplify were verified by sequencing, which demonstrated that the *dps* gene was indeed knocked out from R12 genome, resulting in the *Δdps* R12 mutant.

The *D. wulumuqiensis* R12 growth condition after deletion of *dps* gene

Dps has been shown to play an important role during exponential phase and stationary phase growth in *E. coli* [3]. In this study, we want to investigate the effects ofthe *D. wulumuqiensis* R12 growth after the deletion of *dps* gene. Hence the WT R12 strain and *Δdps* R12 mutant growth curves were measured. As shown in Fig. 4A, the WT R12 strain and *Δdps* R12 mutant both entered to logarithmic phase at 8 h. However, the OD_{600} value of the WT R12 strain was about 2-fold that of the *Δdps* R12 mutant. At 15 h, the WT R12 strain has been in stationary phase with OD_{600} value reached to ~7, while *Δdps* R12 mutant was less than 5 and reached to stationary phase at 21 h. The difference of growth condition indicated that the cell growth of *D. wulumuqiensis* R12 can be affected when the *dps* gene was deleted.

The survival rate of WT R12 strain and *Δdps* R12 mutant under the exposure of UV rays

According to the analyses of Dps structure and sequence, the Dps can bind DNA to protect chromosome through the N-terminal. UV irradiation was used to verify the UV tolerance of *D. wulumuqiensis* R12 was significantly reduced when Dps protein was lost. As shown in Fig. 4B, after 6 min UV irradiation, the survival rate of WT R12 strain was more than 90%, while the *Δdps* R12 mutant was less than 20%. When the irradiation time reached to 12 min, the *Δdps* R12 mutant can not survive on the plate, whereas the survival rate of WT R12 strain was about 80%. We hypothesized that Dps protein in *D. wulumuqiensis* R12 plays a crucial role in protecting DNA.

Sensitivity to H_2O_2 oxidative treatments of WT R12 strain and *Δdps* R12 mutant

The DNA protection experiment *in vitro* in this paper verified that R12 Dps protein can reduce fenton reaction to a certain extent. In order to investigate the role of R12 Dps proteins *in vivo*, the WT R12 strain and *Δdps* R12 mutant were treated with 80 mM H_2O_2 of different treatment time (0, 10, 20, 30, and 50 min). The survival rate of WT R12 strain and *Δdps* R12 mutant was calculated compared to the untreated sample (0 min treatment). As the H_2O_2 treatment time extension (Fig. 4C), the survival rate of WT R12 strain and *Δdps* R12 mutant was decreased, whereas the survival rate of *Δdps* R12 mutant was 35.98% after 10 min H_2O_2 treatment when WT R12 strain maintained 96.52% survival rate. When the H_2O_2

treatment reached to 50 min, the *Δdps* R12 mutant was almost inactived, and WT R12 strain retained 64.44% survival rate that was 8-fold to the *Δdps* R12 mutant. The result suggested that the oxidation resistance ability of *D. wulumuqiensis* R12 would be weaken when the Dps proteins were not exist in cells.

TEM analyses of WT R12 strain and *Δdps* R12 mutant

The cells of *D. wulumuqiensis* R12 were more sensitive to H_2O_2 after the *dps* gene deletion. To explore the specific effects of H_2O_2 on the *Δdps* R12 mutant, the WT R12 strain and *Δdps* R12 mutant were both treated with 80 mM H_2O_2 for 15 min, after which the cells were fixed for TEM observation. As shown in Fig. 5A and 5B, the cell envelope thickness of the WT R12 strain and the *Δdps* R12 mutant was approximately 160 nm under normal conditions, and the observable cell envelope was divided into four layers. However, the cell envelope thickness of WT R12 strain was reduced to about 120 nm after H_2O_2 treatment (Fig. 5C), and the cell envelope was seriously destroyed in *Δdps* R12 mutant (Fig. 5D). The unusually thick cell envelope is the first barrier of *D. wulumuqiensis* R12 against external stresses when faced with a hostile environment. The antioxidant capacity of *D. wulumuqiensis* R12 was significantly reduced when the Dps proteins were not in *D. wulumuqoensis* R12. And previous research showed that N-terminus of *Dr*Dps2 in the *D. radiodurans* can interact with the membrane [33]. We hypothesised that without the protection of Dps protein, the antioxidant capacity of cell envelope would be reduced.

Difference of proteins expression between the WT R12 strain and the *Δdps* R12 mutant

In this study, both WT R12 strain and the *Δdps* R12 mutant were used in triplicate, and each sample was in logarithmic phase, and a total of 1,009 proteins were detected by spectrum search analysis. Among these 116 proteins were up, and 111 were down-regulated, with fold change > 1.5 and p value < 0.05 (Fig. 6). Thus, the numbers of up and down-regulated proteins following *dps* knockout were simliar. In this work, we mainly focused on a series of adverse effects caused by *dps* gene knockout in *D. wulumuqiensis* R12. Therefore, the down-regulated proteins were analyzed further.

GO analysis of differentially expressed proteins in the WT R12 strain and the *Δdps* R12 mutant

To further understand the functional characteristics of the differential expressed proteins, GO enrichment analyses of the categories Cellular Component, Molecular Function, and Biological Process were performed. The up-regulated proteins were enriched for the Cellular Component categories DNA-directed RNA polymerase complex, nucleoid, RNA polymerase. They were also enriched for the molecular functions 5’-3’ RNA polymerase activity, ribonucleoside binding, nucleoside binding, RNA polymerase activity, DNA-directed 5'-3' RNA polymerase activity, nucleotidyltransferase activity, zinc ion binding as well as the Biological Process category hexose catabolic process, galactose metabolic process and monosaccharide catabolic process (Fig. 7A). The down-regulated proteins were enriched in the Cellular Component categories outer membrane-bound periplasmic space, cell envelope, envelope, periplasmic space. They were also enriched in the Molecular Function categories disulfide oxidoreductase activity, cofactor binding, tetrapyrrole binding, heme binding, and zinc ion binding as well as the Biological

Process category carboxylic acid catabolic process (Fig. 7B). Additionally, in down GO term, metabolic process, cellular process, growth, response to stimulus, interspecies interaction between organisms, localization, multi-organism process, biological regulation in Biological Process; cell, intracellular, protein-containing complex in Cellular Component; catalytic activity, binding, antioxidant activity, and molecular carrier activity were in down-regulation (Fig. 7C). Also, in up GO term, the cellular process, metabolic process, response to stimulus, growth, biological regulation (Biological Process); cell, intracellular, protein-containing complex (Cellular Component); and catalytic activity, binding, transporter activity, antioxidant activity, molecular function regulator, and transcription regulator activity (Molecular Function) were in up-regulation (Fig. 7D). These data imply that Dps may influence a large number of proteins with different functions.

The TEM results showed that the cell envelope of the *Δdps* R12 mutant was severely damaged by treatment with 80 mM H_2O_2. Cells of *D. wulumuqiensis* R12 can form tetrads, and possess a thick cell envelope (Fig. 5). The cell envelope of *Deinococcus* exhibits an unusual structure and composition [34], and some *Deinococcus* species have six layers in the cell envelope. The entire *D. radiodurans* cell is enveloped by a dense carbohydrate shell, a thick cellular structure that might contribute to its extreme stress resistance [34-35]. *D. wulumuqiensis* R12 shares similar cell-envelope characteristics, and its envelope is even thicker than that of in *D. radiodurans* [6]. The *Δdps* R12 mutant's proteins in the GO catagory cell envelope were significantly down-regulated, among which the ABC transporter substrate-binding protein, phosphate-binding protein, and thiamine ABC transporter substrate-binding protein were in down-regulation, which might explain why the envelope was more sensitive to H_2O_2 and damaged by the stress treatment.

To investigate the response to oxidative stress in *D. wulumuqiensis* R12, several crucial proteins were analyzed. In the Biological Process and Molecular Function catagories, "response to oxidative stress" GO term, such as the catalase (DVJ83_01425), and dihydrolipoyl dehydrogenase (*lpd*A) were significantly down-regulated. Catalase is a metalloenzyme that detoxifies H_2O_2 into water and O_2, thereby protecting organisms from oxidative damage caused by H_2O_2 [36]. Three catalases (DVJ83_14715, DVJ83_03805 and DVJ83_01425) were identified in *D. wulumuqiensis* R12, the catalases encoded by the DVJ83_14715 and DVJ83_03805 genes were expressed under normal conditions, while catalase DVJ83_01425 was down-regulated. The proteomic data showed that the catalase DVJ83_01425 was down-regulated 2.07-fold in response to chemical, 1.91-fold in cofactor metabolic processes, 2.48-fold in response to oxidative stress, 4.14-fold in nucleoside bisphosphate metabolic process, 5.39-fold in heme binding, and 2.45-fold in cofactor binding. The catalase DVJ83_01425 was in down-regulated when the *dps* gene was knocked out, reducing the antioxidative capacity of *D. wulumuqiensis* R12. Also, we found two catalases (catalase1 and catalase2) in *D. wulumuqiensis* R12 genome, and the catalase2 was significantly down-regulated. These data indicated that the catalases would be affected with the deletion of *dps* gene. Whereas the H_2O_2 tolerance was reduced not only the Dps was lost, but the catalases were down-regulated in *D. wulumuqiensis* R12.

The growth of the *Δdps* R12 mutant was significantly slower than that of the WT strains. ABC substrate-binding transporter were significantly down-regulated. ABC transporters (ATP-binding cassette transporter) are one of the largest and oldest protein families, which plays a crucial role in the physiology of all organisms [37-38]. It uses the energy of ATP hydrolysis to transport a wide range of biomolecules across the membrane [38]. The substrate-binding proteins bind the substrate with high affinity and deliver it to the transporter [39]. ABC importers are major determinants of the acquisition of essential nutrients in bacteria [40-41]. The slow growth of *D. wulumuqiensis* R12 after *dps* gene knock out can be explained by the down-regulation of ABC substrate-binding transporter. In addition, in the down-regulated GO term, the "growth" in Biological Process GO term was down-regulated, among which "Fe-S cluster assembly protein SufB (*suf*B)", "Phosphate transport system permease protein PstA (DVJ83_13895)", "Pyridoxal 5'-phosphate synthase subunit PdxS (*pdx*S)", "Phosphate transport system permease protein (*pst*C)", "Cysteine-tRNA ligase (*cys*S)", "Glycine dehydrogenase (*gcv*P)", and "Elongation factor G (*fus*A)". These proteins were down-regulated that might cause the lower growth of *Δdps* R12 mutant compared to WT R12 strain.

KEGG analysis of differently expressed proteins in the WT R12 strain and the *Δdps* R12 mutant

KEGG (Kyoto Encyclopedia of Gene and Genome) is an information network that connects known molecular interactions such as metabolic pathways, complexes, and biochemical reactions. According to the proteomics data, the map02010 (ABC transporters), map02024 (Quorum Sensing), map03020 (RNA polymerase), map00330 (Arginine and proline metabolism), map00500 (Starch and sucrose metabolism), map00052 (Galactose metabolism), and map00521 (Streptomycin biosynthesis) pathways were significantly enriched (Fig. 8A). By contrast, only the map02024, map02010, and map05512 pathways were down-regulated (Fig. 8B).

The *Δdps* R12 mutant grew slower than the WT R12 strain (Fig. 4A). ABC transporter are the important for the import of nutrients [38]. As shown in Fig. S3A, mineral and organic ion transporters (*Tbp*A); oligosaccharide, polyol, and lipid transporters (*Chi*E, *Bmp*A and *Nup*B); as well as phosphate and amino acid transporters (*Pst*S, *Pst*A, *Pst*C, *Pst*B, *liv*K and *Tcy*A) were down-regulated. ATP-dependent proteins are valuable for the removal of oxidative damages and dysfunctional proteins [42]. These results indicated that Dps may also be important for the growth of *D. wulumuqiensis*.

Bacteria cells can communicate using a cell-density dependent regulatory system known as quorum sensing (QS) [43]. QS is associated with a number of cellular processes, such as motility, biofilm formation or antibiotic production [44-46]. However, the molecular mechanisms underlying QS circuits in many bacterial species remain unclear, while QS might play important roles in the response to environmental stresses in *D. radiodurans* [42]. On the basis of proteomic data (Fig. S3B), the QS KEGG pathway (map02024) was significantly down-regulated, and 9 proteins were mapped, including branched-chain amino acid ABC transporter substrate-binding protein (DVJ83_00750, DVJ83_02800, DVJ83_06100, and DVJ83_07370), a multifunctional fusion protein (*sec*D), and ABC transporter substrate-binding protein (DVJ83_03180, DVJ83_03190, DVJ83_04825, and DVJ83_13605). The

downregulation of these proteins can also help explain the reduced stress resistance of *D. wulumuqiensis* R12 following the knockout of the *dps* gene.

Protein-protein interaction network of differentially expressed proteins

Deletion of the *dps* gene in *D. wulumuqiensis* R12 induced a series of unfavourable phenotypes resulting from the interaction of multiple proteins. Cell growth and antioxidant defenses were decreased when the *dps* gene was deleted. A total of 48 up- and 34 down-regulated proteins were predicted to interact with each other. The protein-protein interaction (PPI) network was divided into 8 modules (A-I) as shown in Fig. 9. The proteins in module A are mainly involved in metabolism. Notably, glyceraldehyde-3-phosphate dehydrogenase (A0A345IFK5), which is a key enzyme in the glycolytic pathway [47], was strongly down-regulated. Dihydrolipoyl dehydrogenase (A0A345II30) is a component of the pyruvate dehydrogenase complex that plays an important role in the decarboxylation of pyruvate to produce acetyl-CoA [48]. Module D contained proteins that are part of the phosphate transport system, and down-regulated proteins were predicted to interact in pairs. Module E was composed of ABC transporter, which was significantly down-regulated. Module I was mainly contained antioxidative enzymes, among which superoxide dismutase (A0A345IKM4) and catalase (A0A345IEC2) were down-regulated in the PPI. These data indicated that the metabolism, transport and oxidation-reduction processes might be affected in *D. wulumuqiensis* R12 when loss of Dps proteins.

Conclusions

In this study, the sequence, structure, and function of Dps in *D. wulumuqiensis* R12 were analyzed, the N-terminal of Dps protein might play an important role in DNA binding or protection. The docking data and DNA binding experiments *in vitro* showed that DNA binding data of R12 Dps is better than that of R1 Dps1. In addition, *Δdps* R12 mutant was constructed, and comparative proteomics was used to investigate the functions of Dps in *D. wulumuqiensis* R12. The qRT-PCR and proteomics data suggested that when the *dps* gene was knocked out in *D. wulumuqiensis* R12, the *catalase* gene was down-regulated. The proteomics data also suggested that that the metabolism, transport and oxidation-reduction processes were down-regulated in *D. wulumuqiensis* R12 after the *dps* gene was knocked out.

Declarations

Acknowledgments

This work was supported by the National Natural Science Foundation of China (31922070, U2106228, 32060004), the Postgraduate Research & Practice Innovation Program of Jiangsu Province (KYCX19_0872), and the Fundamental Research Funds for the Central Universities (0214-14380502).

Competing Interests

Not declared

Ethical Approval

Not required

References

[1] Anderson D, Busch H, Greene H, Simbonis S. Studies on the metabolism of plasma proteins in tumor-bearing rats. Yale J Bio Med. 1955;27:339-349.

[2] Jung KW, Lim SY, Bahn YS. Microbial radiation-resistance mechanisms. J Microbiol. 2017;55:499-507.

[3] Nair S, Finkel SE. Dps protects cells against multiple stresses during stationary phase. J Bacteriol. 2004;186:4192-8.

[4] Qi HZ, Wang WZ, He JH, Ma Y, Xiao FZ, He SY. Antioxidative system of *Deinococcus radiodurans*. Res Microbiol. 2019;2:45-54.

[5] Maqbool I, Ponniresan V, Govindasamy K, Prasad NR. Understanding the survival mechanisms of *Deinococcus radiodurans* against oxidative stress by targeting thioredoxin reductase redox system. Arch Microbiol. 2020;202:2355-2366.

[6] Gao LH, Zhou ZF, Chen XN, Zhang W, Lin M, Chen M. Comparative proteomics analysis reveals new features of the oxidative stress response in the polyextremophilic bacterium *Deinococcus radiodurans*. Microorganisms. 2020;8:451.

[7] Daly MJ. Modulating radiation resistance: Insights based on defenses against reactive oxygen species in the radio-resistant bacterium *Deinococcus radiodurans*. Clin Lab Med. 2006;26:491-504.

[8] Cox MM, Battista JR. *Deinococcus radiodurans*: the consummate survivor. Nat Rev Microbiol. 2005;3:882-892.

[9] Makarova KS, Aravind L, Wolf YI, Tatusov RL, MInton KW, Koonin EV, Daly MJ. Genome of the extremely radiation-resistant bacterium *Deinococcus radiodurans* viewed from the perspective of comparative genomics. Microbiol Mol Biol Rev. 2001;65:44-79.

[10] Jin MM, Xiao AQ, Zhu LY, Zhang ZD, Huang H, Jiang L. The diversity and commonalities of the radiation-resistance mechanisms of *Deinococcus* and its up-to-date applications. AMB Express. 2019;9:138.

[11] Ranawat P, Rawat S. Radiation resistance in thermophiles: mechanisms and applications. World J Microbiol Biotechnol. 2017;33:112.

[12] Peana M, Chasapis CT, Simula G, Medici S, Zoroddu MA. A Model for manganese interaction with *Deinococcus radiodurans* proteome network involved in ROS response and defense. J Trace Elem

Medicine Biol. 2018;50:4654-473.

[13] Zeng Y, Ma Y, Xiao FZ, Wang WZ, He SY. Knockout of *pprM* decreases resistance to desiccation and oxidation in *Deinococcus radiodurans*. Indian J Microbiol. 2017;57:316-321.

[14] Daly MJ. A new perspective on radiation resistance based on *Deinococcus radiodurans*. Nat Rev Microbiol. 2009;7:237-245.

[15] Romão CV, Mitchell EP, Mcsweeney S. The crystal structure of *Deinococcus radiodurans* Dps protein (DR2263) reveals the presence of a novel metal centre in the N terminus. J Biol Inorga Chem. 2006;11:891-902.

[16] Alcntara NRD, Fábio FMD, Garcia W, Stantos OALD, Junqueira-Kipnis AP, Kipnis A. Dps protein is related to resistance of *Mycobacterium abscessus* subsp. *massiliense* against stressful conditions. Appl Microbiol Biotechnol. 2020;104:5065-5080.

[17] Bessonova TA, Shumeiko SA, Purtov YA, Antipov SS, Preobrazhenskaya EV, Tutukina MN, Ozoline ON. Hexuronates influence the oligomeric form of the Dps structural protein of bacterial nucleoid and its ability to bind to linear DNA fragments. Biophysics. 2016;61:825-832.

[18] Cuypers MG, Mithell EP, Romão CV, McSweeney SM. The Crystal Structure of the Dps1 from *Deinococcus radiodurans* reveals an unusual pore profile with a non-specific metal binding site. J Mol Biol. 207;371:787-799.

[19] Tian B, Sun Z, Shen S, Wang H, Jiao J, Wang L, Hu Y, Hua Y. Effects of carotenoids from *Deinococcus radiodurans* on protein oxidation. Lett Appl Microbiol. 2009;49:689-94.

[20] Hanna ES, Roque-Barreira M, Mendes GMT, Soares SG, Brocchi M. Cloning, expression and purification of a glycosylated form of the DNA-binding protein Dps from *Salmonella enterica* Typhimurium. Protnin Expr Purif. 2008;59:197-202.

[21] Calhoun LN, Kwon YM. The ferritin-like protein Dps protects *Salmonella enterica* serotype enteritidis from the fenton-mediated killing mechanism of bactericidal antibiotics. Int J Antimicrob Agents. 2011;37:261-265.

[22] Tian X, Huang L, Wang MS, Biville F, Zhu DK, Jia RY, Chen S, Zhao XX, Yang Q, et al. The functional identification of Dps in oxidative stress resistance and virulence of *Riemerella anatipestifer* CH-1 using a new unmarked gene deletion strategy. Vet Microbiol. 2020;247:108730.

[23] Asker D, Awad TS, Beppu T, Ueda K. *Deinococcus misasensis* and *Deinococcus roseus*, novel members of the genus *Deinococcus*, isolated from a radioactive site in Japan. Syst Appl Microbiol. 2008;31:43-49.

[24] Agostini HJ, Carroll JD, Minton KW. Identification and characterization of uvrA, a DNA repair gene of *Deinococcus radiodurans*. J Bacteriol. 1996;178:6759-6765.

[25] Meima R, Lidstrom ME. Characterization of the minimal replicon of a cryptic *Deinococcusradiodurans* SARK plasmid and development of versatile *Escherichia coli-D. radiodurans* shuttle vectors. Appl Environ Microbiol. 2000;66:3856-3867.

[26] Xu X, Jiang L, Zhang ZD, Shi YH, Huang H. Genome sequence of a gamma- and UV-Ray-Resistant strain, *Deinococcus wulumuqiensis* R1. Genome Announc. 2013;1:e00206-13.

[27] Choi HW, Nesvizhskii AI. False discovery rates and related statistical concepts in mass spectrometry-based proteomics. J Proteome Res. 2008;7:47-50.

[28] Nesvizhskii AI. A survey of computational methods and error rate estimation procedures for peptide and protein identification in shotgun proteomics. J Proteomics. 2010;73:2092-2123.

[29] Käll L, Storey JD, MacCoss MJ, Noble WS. Assigning significance to peptides identified by tandem mass spectrometry using decoy databases. J Proteome Res. 2008;7:29-34.

[30] Benjamini Y, Hochberg Y. Controlling the false discovery rate: a practical and powerful approach to multiple testing. J R Stat SocB. 1995;57:289-300.

[31] Aggarwal S, Yadav AK. False discovery rate estimation in proteomics. Methods Mol Biol. 2016;1362:119-28.

[32] Ceci P, Cellai S, Falvo E, Rivetti C, Rossi GL, Chiancone E. DNA condensation and self-aggregation of *Escherichia coli* Dps are coupled phenomena related to the properties of the N-terminus. Nucleic Acids Res. 2004;32:5935-5944.

[33] Santos SP, Cuypers MG, Round A, Finet S, Narayanan T, Mitchell EP, RomÃO CV. SAXS Structural studies of Dps from *Deinococcus radiodurans* highlights the conformation of the mobile N-terminal extensions. J Mol Biol. 2017;429:667-687.

[34] Gerber E, Bernard R, Castang S, Chabot N, Coze F, Dreux-Zigha A, Hauser E, et al. *Deinococcus* as new chassis for industrial biotechnology: biology, physiology and tools. J Appl Microbiol. 2015;119:1-10.

[35] Makarova KS, Aravind L, Wolf YI, Tatusov RL, Minton KW, Koonin EV, Daly MJ. Genome of the extremely radiation-resistant bacterium *Deinococcus radiodurans* viewed from the perspective of comparative genomics. Microbiol Mol Biol Rev. 2001;65:44-79.

[36] Brioukhanov AL, Netrusov AI, Eggen RIL. The catalase and superoxide dismutase genes are transcriptionally up-regulated upon oxidative stress in the strictly anaerobic archaeon *Methanosarcina barkeri*. Microbiology. 2006;152:1671-1677.

[37] Dassa E, Bouige P. The ABC of ABCS: a phylogenetic and functional classification of ABC systems in living organisms. Res Microbiol. 2001;152:211-29.

[38] Sabrialabe S, Yang JG, Yariv E, Ben-Tal N, Lewinson O. Substrate recognition and ATPase activity of the *E. coli* cysteine/cystine ABC transporter YecSC-FliY. J Biol Chem. 2020;295:5245-5256.

[39] Berntsson RP, Smits SHJ, Schmitt L, Slotboom D, Poolman B. A structural classification of substrate-binding proteins. FEBS Lett. 2010;5842606-2617.

[40] Kadaba NS, Kaiser JT, Johnson E, Lee A, Rees DC. The high-affinity *E. coli* methionine ABC transporter: structure and allosteric regulation. Science. 2008;321:250-253.

[41] Rohrbach MR, Braun V, Köster W. Ferrichrome transport in *Escherichia coli* K-12: altered substrate specificity of mutated periplasmic FhuD and interaction of FhuD with the integral membrane protein FhuB. J Bacteriol. 1995;177:7186-7193.

[42] Lin L, Dai S, Tian B, Li T, Yu JL, Liu CZ, Wang LY, Xu H, Zhao Y, Hua YJ. DqsIR quorum sensing-mediated gene regulation of the extremophilic bacterium *Deinococcus radiodurans* in response to oxidative stress. Mol Microbiol. 2006;100:527-41.

[43] Fuqua WC, Winans SC, Greenberg EP. Quorum sensing in bacteria: the LuxR-LuxI family of cell density-responsive transcriptional regulators. J Bacteriol. 1994;176:269-275.

[44] Swift S, Downie JA, Whitehead NA, Barnard AM, Salmond GP, Williams P. Quorum sensing as a population-density-dependent determinant of bacterial physiology. Adv Microb Physiol. 2001;45:199-270.

[45] Waters CM, Bassler BL. Quorum sensing: cell-to-cell communication in bacteria. Annu Rev Cell Dev Biol. 2005;21:319-346.

[46] Williams P. Quorum sensing, communication and cross-kingdom signalling in the bacterial world. Microbiology. 2007;153:3923-3938.

[47] Leu JI, Murphy ME, George DL. Functional interplay among thiol-based redox signaling, metabolism, and ferroptosis unveiled by a genetic variant of TP53. Proc Natl Acad Sci U S A. 2020;117:26804-26811.

[48] Wenk S, Schann K, He H, Rainaldi V, Kim S, Lindner SN, Bar-Even A. An “energy-auxotroph” *Escherichia coli* provides an in vivo platform for assessing NADH regeneration systems. Biotechnol Bioeng. 2020;117:3422-3434.

Figures

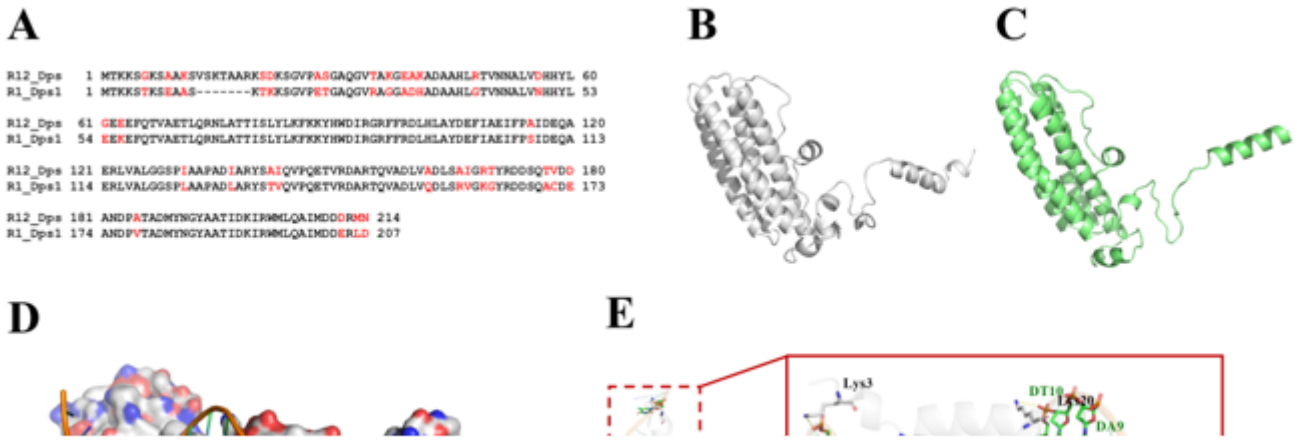

Figure 1

Sequence alignment and structure analyses between of R12 Dps and R1 Dps1. (A) The sequence alignment between R12 Dps and R1 Dps1. (B) R12 Dps model built by RoseTTAFold. (C) The R1 Dps1 model repaired by RosettaFold which the original structure was 2C2F (PDB code). (D) The docking result between R12 Dps and DNA. (E) Hydrogen bonds between R12 Dps protein and DNA. (F) The docking result of R1 Dps1/DNA. (G) Hydrogen bonds between R1 Dps1 and DNA.

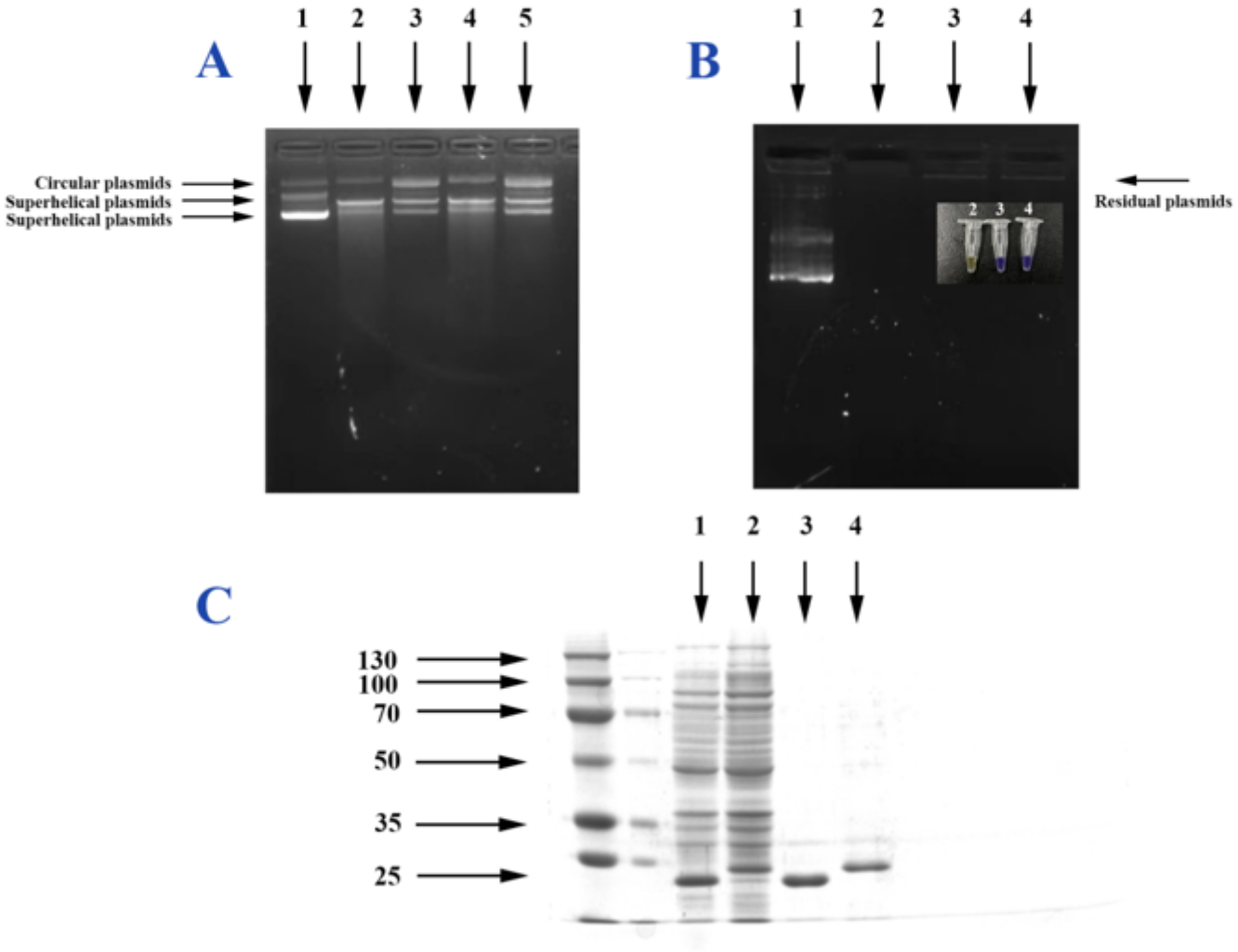

Figure 2

The purification of R12 Dps and R1 Dps1 proteins. (A) The DNA binding tests of R12 Dps and R1 Dps1 proteins. Lane 1: pET-22b(+) plasmids; Lane 2: The plasmids combined with R1 Dps1 proteins (crosslinked with deionized water); Lane 3: The plasmids combined with R12 Dps proteins (crosslinked with deionized water); Lane 4: The plasmids combined with R1 Dps1 proteins (crosslinked with 0.1% glutaraldehyde); Lane 5: The plasmids combined with R12 Dps proteins (crosslinked with 0.1% glutaraldehyde). (B) The DNA protection experiments of R12 Dps and R1 Dps1 proteins. Lane 1: pET-22b(+) plasmids; Lane 2: The resulting plasmid attacked with 80 mM H_2O_2; Lane 3: The resulting plasmid attacked with 80 mM H_2O_2 with the protection of the R1 Dps1 protein; Lane 4: The resulting plasmid attacked with 80 mM H_2O_2 with the protection of the R12 Dps protein; (C) The purification of R1 Dps1 and R12 Dps proteins. Lane 1: The crude enzymes of pET-22b(+)-R1Dps1 recombinant *E. coli.* Lane 2: The crude enzymes of pET-22b(+)-R12Dps recombinant *E. coli.* Lane 3: The purified R1 Dps1 protein; Lane 4: The purified R12 Dps protein.

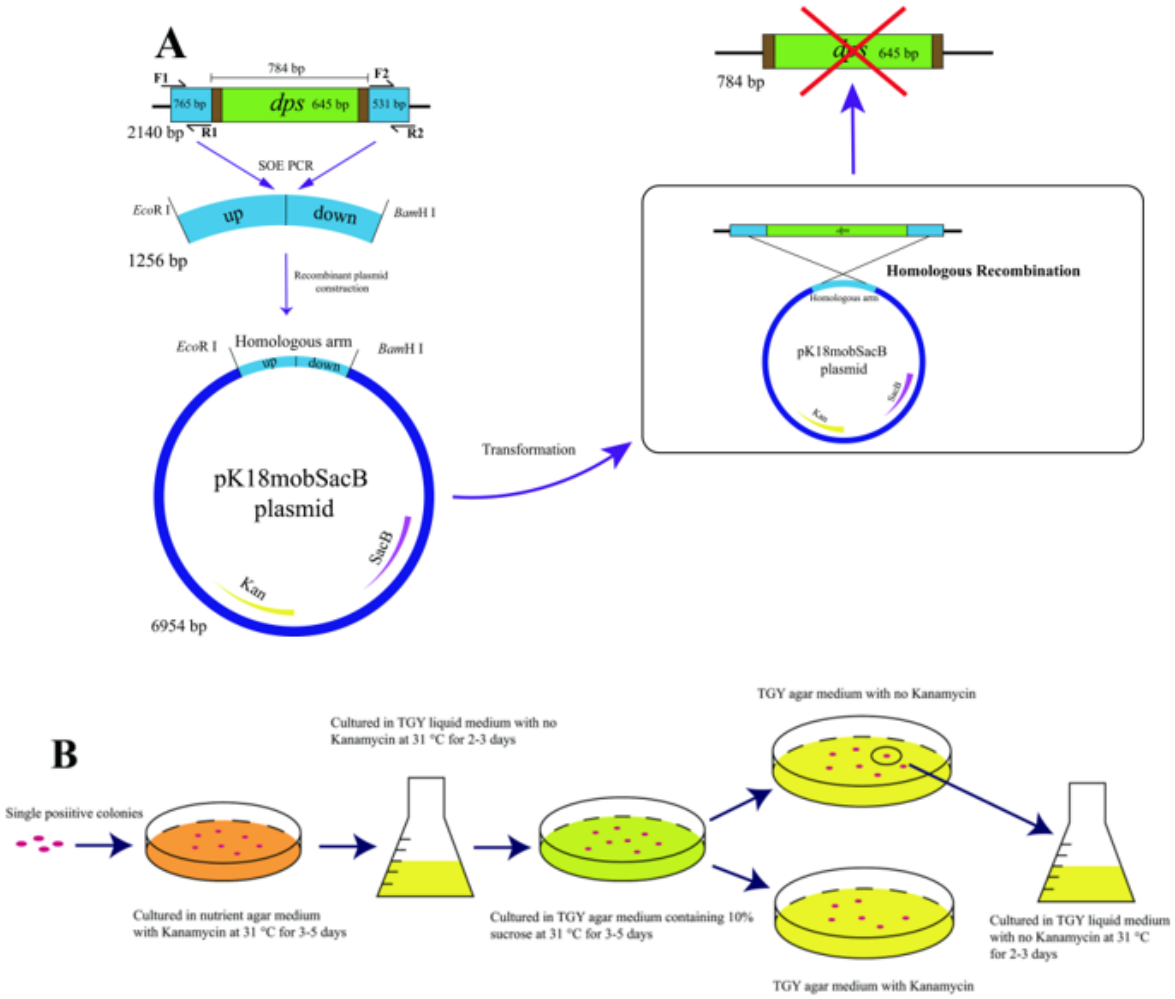

Figure 3

The process of obtaining *Δdps* R12 mutant. (A) Homologous recombination to knock out *dps* gene. (B) The screening of *Δdps* R12 mutant positive colony.

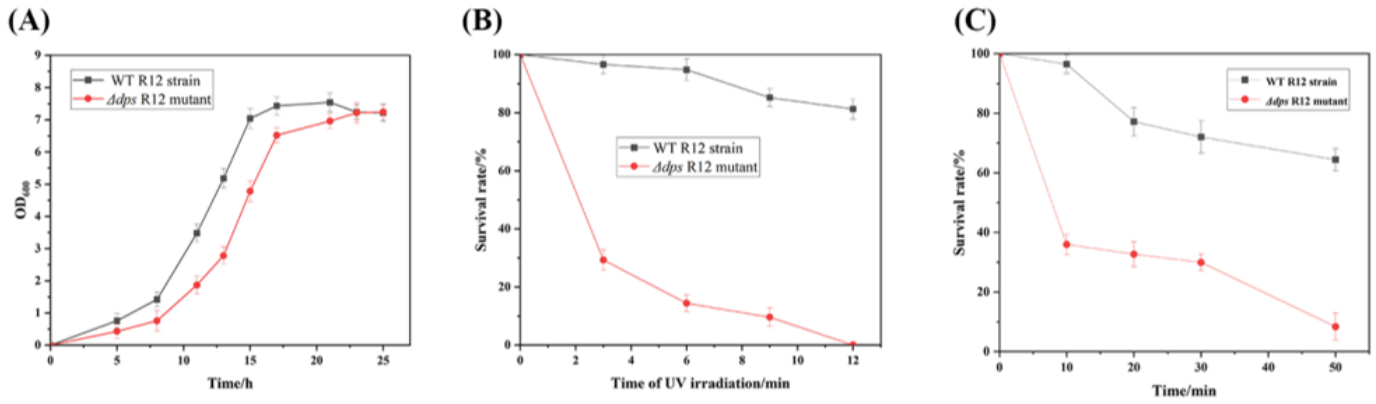

Figure 4

(A) The growth curve of WT R12 strain and *Δdps* R12 mutant measured with the temperature 31 °C for 25 h. (B) The survival rate of WT R12 strain and *Δdps* R12 mutant after 0, 3, 6, 9, 12 min 700 J m^{-2} UV irradiation. (C) The survival rate of WT R12 strain and *Δdps* R12 mutant under different time H_2O_2 treatment.

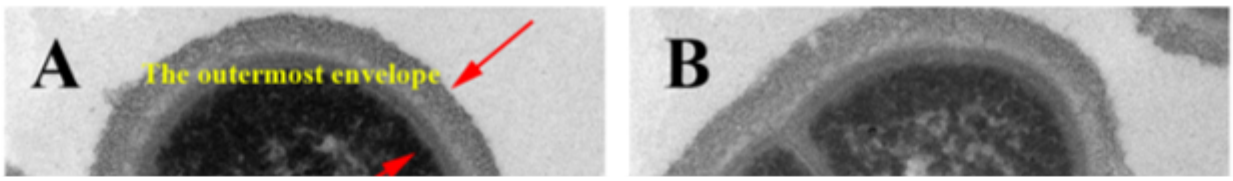

Figure 5

The TEM analyses of WT R12 strain and *Δdps* R12 mutant after treated with 80 mM H_2O_2 for 15 min. (A) The WT R12 strain was in normal growth condition. (B) The *Δdps* R12 mutant in normal growth condition. (C) The WT R12 strain with treated with H_2O_2. (D) The *Δdps* R12 mutant after H_2O_2 treatment.

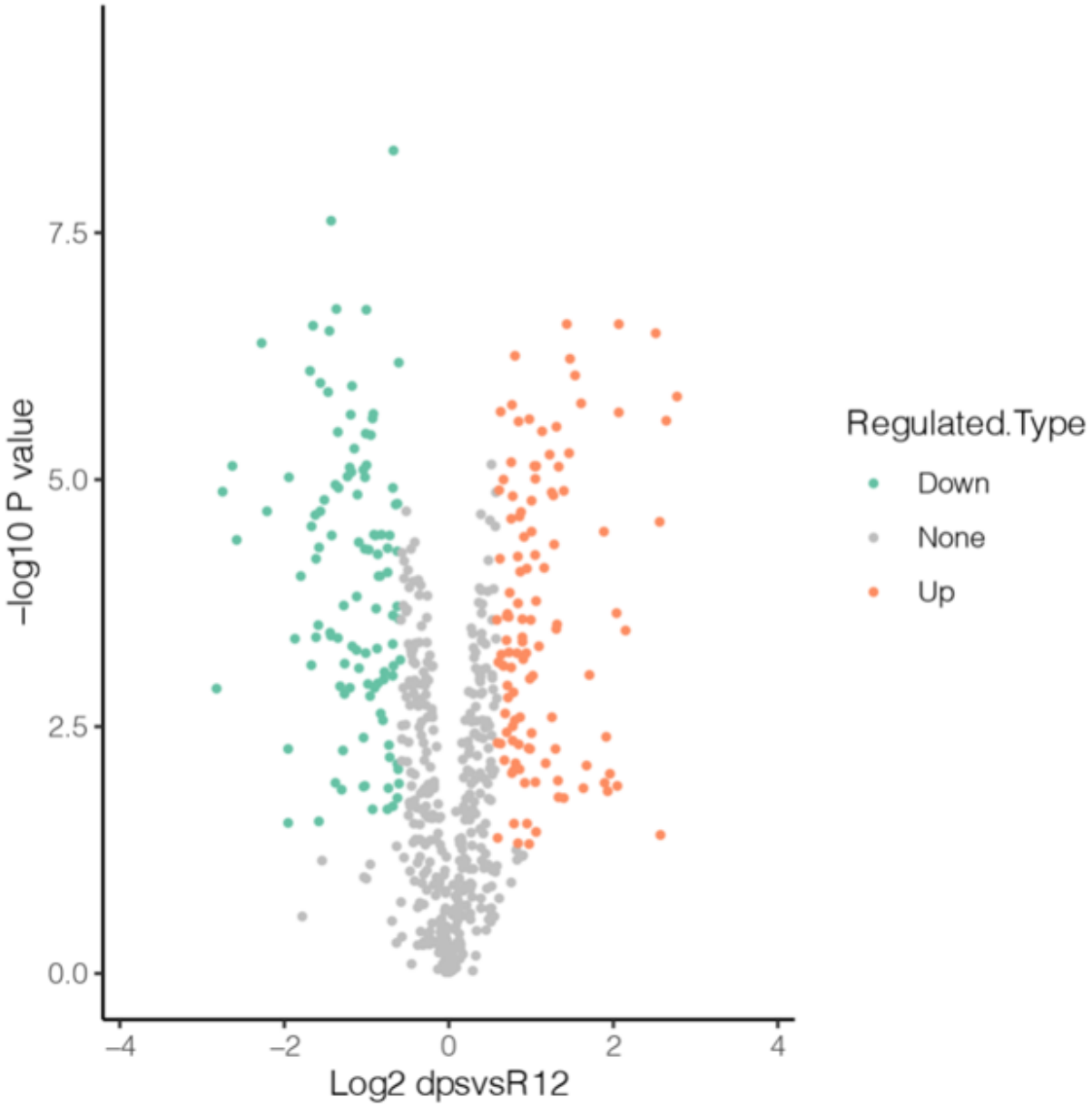

Figure 6

The differential protein volcano plot, the relative quantitative value of protein needs to undergo Log2 logarithmic conversion, and the *p* value was converted to Log10 value. The proteins detected in WT R12 strain and *Δdps* R12 mutant are shown. Each point represents a protein. The orange points suggest up-regulated proteins, and the green points indicate down-regulated proteins in *Δdps* R12 mutant.

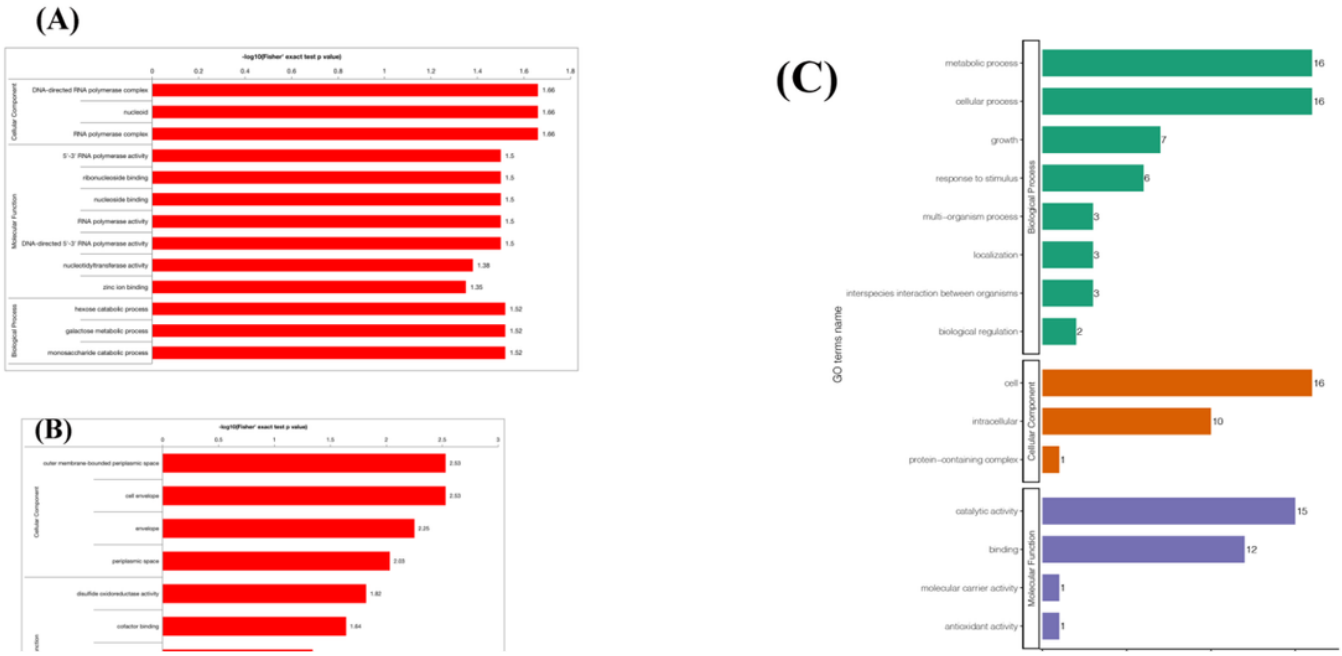

Figure 7

The GO analyses between *Δdps* R12 mutant and WT R12 strain. (A) The up enrichment GO description in *Δdps* R12 mutant. (B) The down enrichment GO description in *Δdps* R12 mutant. (C) The down GO term in *Δdps* R12 mutant. (D) The up GO term in *Δdps* R12 mutant.

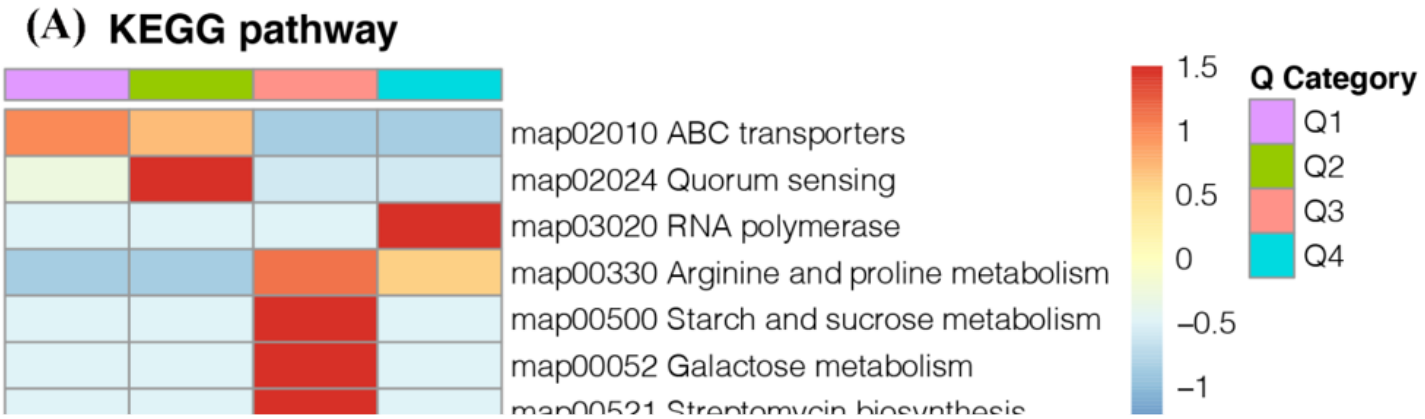

Figure 8

The KEGG enrichment and down-regulated pathways. (A) The heatmap of KEGG pathway according to the *P* value of Fisher's exact test obtained from enrichment analysis, the related functions in different groups were grouped together using hierarchical clustering method. The horizontal axis of the heatmap represents the enrichment test results of different groups, while the vertical axis represents the differentially expressed enrichment related functions. The Q1-Q4 represent differentially expressed multiples [Q1 (< 0.5); Q2 (0.5-0.667); Q3 (1.5-2); Q4 (>2)]. (B) The bubble chart of down-regulated KEGG. The circle color indicates the enrichment significance *P*-value, while the circle size is the number of different proteins in the functional class.

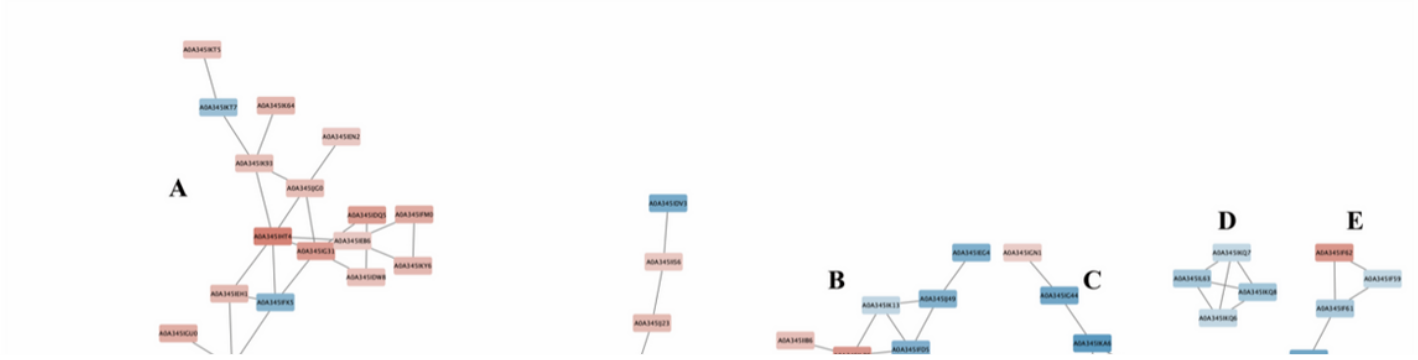

Figure 9

The protein-protein interaction (PPI) network in *D. wulumuqiensis* R12 revealed by functional protein association network (STRING) analysis. A total of 82 differential proteins were shown in PPI network. The up-regulated proteins were shown with red, and proteins in down-regulation was blue.

Supplementary Files

This is a list of supplementary files associated with this preprint. Click to download.

- GOTermsLevel2Classify.xlsx
- GOenrichment.xlsx
- MSidentifiedinformation.xlsx
- SupplementaryMaterial.docx